RESEARCH ARTICLE

Metamaterial acoustics on the Poincaré disk

Michael M. Tung

[1]Instituto de Matemática Multidisciplinar, Universitat Politècnica de València, Camino de Vera s/n, 46022 Valencia, Spain

Correspondence
Michael M. Tung. Email: mtung@mat.upv.es

Summary

Historically, the Poincaré disk model has taken a pioneering role in the development of non-Euclidean geometry. But still today, this model is critical as a playground for simulations and new theories. In this paper, we discuss how to implement and simulate acoustic wave phenomena on the Poincaré disk with the help of so-called metamaterials. After formally developing a theory based on the acoustic potential for the curved spacetime of the Poincaré model, we also provide practical instructions on how to manufacture the appropriate metadevice in a laboratory environment. Finally, as an example, analytical results for the non-trivial radial contributions in concentric wave propagation are derived and the corresponding numerical predictions presented.

KEYWORDS:
applications of local differential geometry to the sciences, relativity and gravitational theory, traveling wave solutions, acoustic analogue models of gravity, Poincaré disk, variational principles of mathematical physics

1 | INTRODUCTION

The discovery that alternative geometries to Euclid's exist and are just as self-consistent, had a profound impact on the concepts of mathematics but also—with the advent of general relativity—on our understanding of the physical universe. Models of hyperbolic geometry are historic landmarks and were crucial for the development and emancipation of geometries other than Euclid's. On a cultural level, tessellations of the hyperbolic plane initiated an artistic revolution in its own way, mutually inspiring mathematics and arts.[1] In today's research, for a wide range of scientific disciplines, elementary hyperbolic geometry in the plane continues to provide an attractive testing ground for diverse and novel theories—in the present case for gravity analogue models of acoustics.[2,3,4,5]

The Poincaré disk model is a straightforward model of hyperbolic geometry on the 2-dimensional disk[6], representing thus one of the simplest case of non-Euclidean geometry with constant negative curvature. It takes over certain properties from the Poincaré half-plane[7,8], but obviously possesses a distinct topology and further symmetry properties. For the disk, the associated metric weighs radial distances from the center of the disk to its circumference in a characteristic manner, thereby contrasting plain Euclidean behavior.

This particular geometry and topology make it a formidable candidate for acoustic wave simulation with metamaterial devices—devices composed of extraordinary materials which allow to implement curved background spacetimes in acoustics.[3,5,9,10,11] As we shall see, not only from the mathematical viewpoint has this model fundamental relevance, but we will argue that its prominent feature can be interpreted as somewhat that of a black hole turned upside down, a quality absent from the related half-plane analogue.[12]

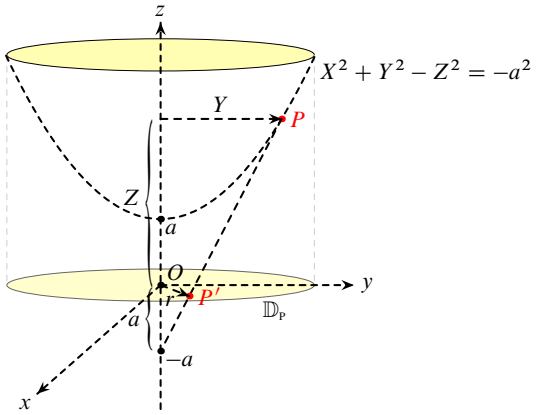

FIGURE 1 Schematic view of the stereographic projection of point P on the upper sheet of a circular hyperboloid to point P' located on the plane $z = 0$. The projection gives the Poincaré disk, $\mathbb{D}_P$, endowed with a characteristic metric, *viz.* Eq. (7).

In this work we study the feasibility to implement acoustics on the Poincaré disk and investigate the wave propagation in such a medium. We explore the main differential-geometric features of this spacetime with its asymptotic behavior and causal boundaries very much alike to those of acoustic black holes.[11] By employing the framework developed before[3,9], we find the acoustic laboratory parameters (mass-density tensor and bulk modulus) corresponding to the underlying spacetime structure. Furthermore, we derive the equations of motion which govern acoustic wave propagation on the Poincaré disk. For better illustration, we present numerical simulations in a variety of scenarios.

The plan of this article is sketched as follows: Section 2 recalls the geometric essentials of the Poincaré disk based on a stereographic projection and thereby introduces the necessary definitions and notations. The 2D metric of the underlying hyperbolic geometry is generalized to (2 + 1)D curved spacetime, as required for the formalism of the subsequent sections. Section 3 outlines how to construct the Poincaré model in two different ways, either gravitationally by predicting the necessary matter-energy content to deform physical spacetime, or via a analogue model of gravity for metamaterial acoustics, thereby deforming acoustic space accordingly to conform with the hyperbolic geometry of the Poincaré disk. Also some particularly interesting geometric characteristics of this spacetime are summarized. Section 4 supplies various examples for wave propagation on the Poincaré disk, using as far as we can get fully analytical results or efficient approximating functions in these toy models. Section 5 is a brief conclusion to round up the discussion.

2 | SPACETIME GEOMETRY

The Poincaré disk, henceforth denoted by $\mathbb{D}_P$, is the resulting image of the stereographic projection $(X, Y, Z) \mapsto (x, y)$ of the upper part of a circular hyperboloid of two sheets, represented by the equation $X^2 + Y^2 - Z^2 = -a^2$, onto the xy-plane.

Figure 1 provides a schematic view of the stereographic mapping, and shows the similar triangles to yield the following relations between the coordinates of the hyperboloid and its projection to the plane, *i.e.*

$$\frac{x}{a} = \frac{X}{Z + a}, \quad \frac{y}{a} = \frac{Y}{Z + a}. \tag{1}$$

Using the conventional radial polar coordinate r on the xy-plane, it is not difficult to find

$$\left.\begin{aligned} X &= \frac{2x}{1 - r^2/a^2} \\ Y &= \frac{2y}{1 - r^2/a^2} \\ Z &= \frac{1 + r^2/a^2}{1 - r^2/a^2}\, a \end{aligned}\right\} \quad \text{for} \quad 0 \le r < a, \tag{2}$$

This induces the following spatial line element for distances ℓ on Poincaré disk $\mathbb{D}_{\text{P}}$:

$$d\ell^2 = dX^2 + dY^2 = 4\frac{dx^2 + dy^2}{\left(1 - r^2/a^2\right)^2}, \tag{3}$$

which in polar coordinates takes the form

$$d\ell^2 = \underbrace{\frac{4dr^2}{\left(1 - r^2/a^2\right)^2}}_{=:\, a^2 d\varrho^2} + \frac{4r^2 d\varphi^2}{\left(1 - r^2/a^2\right)^2}. \tag{4}$$

Here, in Eq. (4), it is customary to introduce the geodesic radius ϱ, which is dimensionless and defined by the integral

$$\varrho = \frac{2}{a}\int_0^r \frac{dr}{1 - r^2/a^2} = \ln\left(\frac{a+r}{a-r}\right) = 2\,\text{artanh}(r/a) \geq 0, \tag{5}$$

and sometimes also called the Poincaré geodesic distance from the origin.[13] This straightforwardly implies the following practical relations

$$e^{\varrho} = \frac{a+r}{a-r} \quad \Rightarrow \quad r = a\,\frac{e^{\varrho} - 1}{e^{\varrho} + 1} \quad \Rightarrow \quad \frac{2r}{1 - r^2/a^2} = a\,\frac{e^{\varrho} - e^{-\varrho}}{2} = a\sinh\varrho \tag{6}$$

which will be of future use, and also immediately converts Eq. (4) to the much simpler form

$$d\ell^2 = a^2 d\varrho^2 + a^2\sinh^2\varrho\, d\varphi^2. \tag{7}$$

Note that Eq. (7) represents the metric of hyperbolic geometry underlying much of the famous artwork by the Dutch artist M.C. Escher.[1] Moreover, it is not difficult to see that $\mathbb{D}_{\text{P}}$ is conformally flat with the conformal factor $\Omega = (1 - r^2/a^2)/2$.

For a relativistic treatment, it now only remains to add the time component, so that the full spacetime metric for the Lorentzian manifold $M = \mathbb{D}_{\text{P}} \times \mathbb{R}$ is given by

$$\boldsymbol{g} = -(cdt) \otimes \underbrace{(cdt)}_{\theta^0} + (ad\varrho) \otimes \underbrace{(ad\varrho)}_{\theta^1} + (a\sinh\varrho\, d\varphi) \otimes \underbrace{(a\sinh\varrho\, d\varphi)}_{\theta^2}, \tag{8}$$

where θ^{μ} ($\mu = 0, 1, 2$) indicates the dual-base forms of the local coframe. Note that in the remainder of the text, all relevant tensor components evaluated in the local coframe will be marked with an additional circumflex symbol. Further, observe that $a > 0$ is a fixed physical length scale, and recall that ϱ, φ are the geodesic polar coordinates. Moreover, $c > 0$ is a constant speed.

This completes the spacetime setup with $M = \mathbb{D}_{\text{P}} \times \mathbb{R}$, and provides all the formal prerequisites necessary for the subsequent simulation of acoustic wave propagation on the Poincaré disk.

3 | MODEL CONSTRUCTION

3.1 | Physical spacetime

In combination with Cartan's structure equations, the dual base $\{\theta^0, \theta^1, \theta^2\}$ introduced by Eq. (8) allows to straightforwardly compute the Riemann curvature tensor $\widehat{R}^{\alpha}{}_{\beta\gamma\delta}$ in the coframe of manifold $M = \mathbb{D}_{\text{P}} \times \mathbb{R}$.

In the nonholonomic frame $(\theta^0, \theta^1, \theta^2)$ local flatness and orthogonality hold satisfying $\widehat{\boldsymbol{g}} = -\theta^0\otimes\theta^0 + \theta^1\otimes\theta^1 + \theta^2\otimes\theta^2$, where $\widehat{\boldsymbol{g}}$ has the signature of a local Minkowski metric. Within Cartan's formalism the computation of the corresponding curvature forms ω and Ω carries through in a straightforward manner. These explicit results for the curvature forms associated with $M = \mathbb{D}_{\text{P}} \times \mathbb{R}$ are required to furnish additional constraints on the spacetime structure under consideration, and thus will eventually give shape to the acoustic model.

First, Cartan's first structure equation expresses that the pseudo-Riemannian geometry, in this case manifold $\mathbb{D}_{\text{P}} \times \mathbb{R}$, is torsion-free so that the exterior covariant derivatives of the dual-base forms vanishes, *i.e.* $D\theta^{\mu} = d\theta^{\mu} + \omega^{\mu}{}_{\nu} \wedge \theta^{\nu} = 0$. Then, for the particular metric, given by Eq. (8), a simple calculation produces the following components for the curvature 1-forms:

$$\omega^{\mu}{}_{\nu} = \begin{pmatrix} 0 & 0 & 0 \\ 0 & 0 & -\frac{1}{a}\coth\varrho\;\theta^2 \\ 0 & \frac{1}{a}\coth\varrho\;\theta^2 & 0 \end{pmatrix}. \tag{9}$$

Second, by applying once more the exterior derivative to Eq. (9), Cartan's second structure equation, *i.e.* $\Omega^{\mu}{}_{\nu} = d\omega^{\mu}{}_{\nu} + \omega^{\mu}{}_{\lambda} \wedge \omega^{\lambda}{}_{\nu}$. yields the curvature 2-forms:

$$\Omega^{\mu}{}_{\nu} = \begin{pmatrix} 0 & 0 & 0 \\ 0 & 0 & -\frac{1}{a^2}\theta^1 \wedge \theta^2 \\ 0 & \frac{1}{a^2}\theta^1 \wedge \theta^2 & 0 \end{pmatrix}, \tag{10}$$

where the only non-zero and independent component is

$$\Omega^{1}{}_{2} = d\omega^{1}{}_{2} = -\theta^1 \wedge \theta^2/a^2 =: \widehat{R}^{1}{}_{212}\,\theta^1 \wedge \theta^2. \tag{11}$$

This easily identifies the only non-vanishing component of the Riemann curvature tensor in the nonholonomic base to be

$$\widehat{R}^{1}{}_{212} = -\frac{1}{a^2}. \tag{12}$$

Performing the usual contraction in Eq. (12) (between the first contravariant and the third covariant index), we obtain the Ricci tensor (in the nonholonomic basis)

$$\widehat{\boldsymbol{R}} = -\frac{1}{a^2}\Big[\theta^1 \otimes \theta^1 + \theta^2 \otimes \theta^2\Big], \tag{13}$$

and next taking the trace, we obtain the Ricci scalar (for all frames)

$$R = -\frac{2}{a^2}. \tag{14}$$

Finally, for determining the necessary physical requirements of $M = \mathbb{D}_{\text{P}} \times \mathbb{R}$, we calculate the Einstein tensor via the expression

$$\widehat{\boldsymbol{G}} = \widehat{\boldsymbol{R}} - \tfrac{1}{2} R\,\widehat{\boldsymbol{g}}, \tag{15}$$

which gives

$$\widehat{G}_{00} = -\frac{1}{a^2}, \quad \widehat{G}_{\mu\nu} = 0 \text{ for } \mu, \nu \neq 0. \tag{16}$$

Note that for the corresponding Einstein tensor $\widehat{G}_{\alpha\beta}$, the 00-component in the local coframe and coordinate frame are identical, which amounts to $\widehat{\boldsymbol{G}} = \boldsymbol{G}$ for this particular spacetime.

As an immediate consequence of the results Eq. (16), the spacetime manifold $M = \mathbb{D}_{\text{P}} \times \mathbb{R}$ displays absence of shear stress and pressure, whereas the underlying energy-matter density ρ_0 is exotic:

$$\underbrace{G_{00}}_{-1/a^2} = \frac{8\pi G}{c^4} \underbrace{T_{00}}_{\rho_0 c^2} \quad \Rightarrow \quad \rho_0 = -\frac{c^2}{8\pi G a^2} < 0. \tag{17}$$

Here, G is the usual gravitational constant. Observe that if the disk extends to infinity, *viz.* $a \to \infty$, the energy-matter content will vanish and M becomes asymptotically flat, which intuitively is expected.

Other important spacetime properties are contained in objects such as the Schouten tensor and the Kretschmann scalar. For example, in the coframe, the Schouten tensor takes the form

$$\widehat{\boldsymbol{S}} = \widehat{\boldsymbol{R}} - \tfrac{1}{4} R\,\widehat{\boldsymbol{g}},$$

which with Eqs. (13) and (14) leads to

$$\widehat{\boldsymbol{S}} = -\frac{1}{2a^2}\Big[\theta^0 \otimes \theta^0 + \theta^1 \otimes \theta^1 + \theta^2 \otimes \theta^2\Big], \tag{18}$$

meaning that the Cotton tensor[14] vanishes, thus again proving conformal flatness for the $(2+1)D$ spacetime extension of Eq. (7). Moreover, if $(2+1)D$ conformal flatness holds, the Kretschmann scalar, which is the quadratic invariant composed of the Riemann tensor, $K = R^{\lambda\mu\nu\rho} R_{\lambda\mu\nu\rho}$, conveniently is given by[11]

$$K = 4\widehat{R}_{\mu\nu}\widehat{R}^{\mu\nu} - R^2,$$

and for the present Poincaré model it readily evaluates to

$$K = \frac{4}{a^4}. \tag{19}$$

The Kretschmann invariant would at least for one spacetime point in M be infinite if the geometry possessed any curvature singularities. Since $a > 0$, this certainly will never occur, and therefore $M = \mathbb{D}_{\text{P}} \times \mathbb{R}$ is singularity free.

Obviously, physical systems with negative energy-matter content, *viz.* Eq. (17), cannot be manufactured and manipulated in current—and likely any advanced—technology, which demonstrates the fundamental impossibility to reproduce spacetime $\boldsymbol{M} = \mathbb{D}_{\mathrm{p}} \times \mathbb{R}$ within conventional, that is, gravitational engineering. Nonetheless, in the following section, we will carry on with the implementation of spacetime $\boldsymbol{M}$ for acoustic metamaterials and show that this is feasible, offering a viable prescription on how to proceed in a laboratory setting.

3.2 | Acoustic gravity analogue

Analog models of gravity [15] aim to transfer the spacetime approach of general relativity to phenomena of other physical domains which at first sight appear to be unrelated with gravity. In a similar fashion as energy-matter deforms and acts on spacetime in relativity, analogue models attempt to identify parameters in their relevant system which distort or shape their own physical space, thereby making it possible to simulate relativistic objects and effects (such as *e.g.* black holes with event horizons) in a real-life laboratory environment. Metadevices—devices built from metamaterials—are in this process the prime choice for the practitioner. During the last two decades many remarkable and decisive theoretical and experimental advances have been accomplished in this field of research. [16,17,18]

Metamaterials are artificial materials engineered in the laboratory endowing them with physical characteristics far beyond those found in nature. With optical metamaterials, for example, it is nowadays possible to manufacture special devices with negative refractive index [19], or superlenses which defy the diffraction limit irrevocably present in conventional lenses. [20,21] Furthermore, cloaking devices which render invisible partially or completely any object, furnish other significant and intriguing applications. [22,23] With metamaterials, researchers and engineers alike are presented with unique possibilities for the development of such novel devices and are apt to propel technological advances.

In this context, acoustic metamaterials allow to model sophisticated acoustic phenomena with curved background spacetimes and make predictions for future laboratory experiments. Likely the most powerful approach to describe such phenomena is the principle of least action, having the advantage to work in a coordinate independent manner and to easily allow the incorporation of differential-geometric techniques in compact form. Working in an invariant manner with respect to arbitrary transformations of the coordinates also entails efficiency—already in classical mechanics Newton's dynamic law for a one-particle system comprises three equations, whereas the Lagrangian formalism consists of only one scalar expression.

For our purposes, let acoustic phenomena be governed by the following elementary variational principle, namely that for spacetime $\boldsymbol{M}$, endowed with metric $\boldsymbol{g}$, the subsequent action will be stationary with respect to variations of the acoustic potential $\phi : \boldsymbol{M} \to \mathbb{R}$, such that integration over bounded spacetime domain $\Omega \subseteq \boldsymbol{M}$ satisfies [3]:

$$\frac{\delta}{\delta \phi} \int_{\Omega} d\mathrm{vol}_g \, \tfrac{1}{2} \boldsymbol{g}(\nabla \phi, \nabla \phi) = 0, \tag{20}$$

Here, $d\mathrm{vol}_g = \sqrt{-g}\, dx^0 \wedge \ldots \wedge dx^3$ is the invariant volume element with $g = \det \boldsymbol{g} < 0$. The Lagrangian density function is therefore

$$\mathscr{L}(\nabla \phi) = \tfrac{1}{2} \boldsymbol{g}(\nabla \phi, \nabla \phi) = \tfrac{1}{2} g^{\mu\nu} \phi_{,\mu} \phi_{,\nu}. \tag{21}$$

The factor $1/2$ is purely conventional (and obviously of no relevance in Eq. (20)), chosen to be consistent with the acoustic Lagrangian in standard format. [24]

In previous work [3], using the conventional acoustic Lagrangian and Eq. (21), we have shown that there exists a general 1-to-1 correspondence between spacetime metric $\boldsymbol{g}$ and the parameters κ (bulk modulus) and $\boldsymbol{\rho}$ (density tensor) of an acoustic metamaterial device. Specifically, in the laboratory (*physical space*), the acoustic engineer wishes to implement a $(2+1)$D spacetime $(\boldsymbol{M}, \boldsymbol{g})$ by calibrating the mass-density tensor ϱ and bulk modulus κ. In doing so, he has to relate these parameters to their values in the corresponding space with known acoustic wave propagation (*virtual space*), denoted by $\widetilde{\varrho}$ and $\widetilde{\kappa}$, respectively. Similarly, following convention, the contravariant spatial components of the metric in virtual space are denoted by $\widetilde{g}^{ij}$, with $i, j = 1, 2$. Then, both physical and virtual spaces are explicitly linked by the so-called *constitutive relations* [3]:

$$\kappa = \frac{\sqrt{\gamma}}{\sqrt{\widetilde{\gamma}}}\, \widetilde{\kappa}, \qquad \rho_0 \rho^{ij} = \frac{\sqrt{\widetilde{\gamma}}}{\sqrt{\gamma}}\, \widetilde{g}^{ij}, \tag{22}$$

where $\gamma = \det\left(g^{ij}\right)$ is the determinant of the spatial metric.

For the case of the Poincaré disk, we substitute Eq. (3) corresponding to

$$g_{ij} = \frac{4}{\left(1 - r^2/a^2\right)^2} \begin{pmatrix} 1 & 0 \\ 0 & 1 \end{pmatrix}, \quad \sqrt{\gamma} = \frac{4}{\left(1 - r^2/a^2\right)^2}$$

into Eq. (22) to obtain

$$\kappa = \frac{4}{\left(1 - r^2/a^2\right)^2} \kappa_0, \quad \rho_0 \rho^{ij} = \tfrac{1}{4} \left(1 - r^2/a^2\right)^2 \begin{pmatrix} 1 & 0 \\ 0 & 1 \end{pmatrix}, \quad 0 \le r < a. \tag{23}$$

Note that the constants κ_0 and ρ_0 (measured in units of Pascal) are fixed by the physical properties of the corresponding flat space, since as virtual space we identified 2D Minkowskian space (with well-defined properties) by taking $\widetilde{\boldsymbol{g}}$ to be the 2×2 identity matrix. This, of course, also implies $\sqrt{\widetilde{\gamma}} = 1$.

Eq. (23) achieves the goal at hand, providing a prescription for simulating acoustic phenomena with underlying spacetime geometry $M = \mathbb{D}_{\text{P}} \times \mathbb{R}$ by fine-tuning the acoustic parameters of a suitable metamaterial.

4 | WAVE SIMULATION

After completing in Section 3.2 the discussion of the specific implementation of $M = \mathbb{D}_{\text{P}} \times \mathbb{R}$ for an acoustic metamaterial, we now proceed to the simulation of wave propagation in such a transmission medium.

The Euler-Lagrange equation for the variational principle, Eq. (20), is

$$* \, d * d\phi = 0, \tag{24}$$

where $*$ is the Hodge dual.[25] Eq. (24) represents the equation of motion for the acoustic potential ϕ that fully determines the physical behavior of the system. In local coordinates, Eq. (24) takes the form of the source-free wave equation $\Delta_M \phi = 0$, with the Laplace-Beltrami Δ_M operator for the curved spacetime background M. Adopting the local coframe in Eq.(8) with the dual-base forms $\theta^0 = c\, dt, \theta^1 = a\, d\varrho$ and $\theta^2 = a \sinh \varrho \, d\varphi$, for Eq. (24) after a lengthy but straightforward computation we obtain

$$-\frac{1}{c^2} \frac{\partial^2 \phi}{\partial t^2} + \frac{1}{a^2} \left(\coth \varrho \, \frac{\partial}{\partial \varrho} + \frac{\partial^2}{\partial \varrho^2} \right) \phi + \frac{1}{a^2 \sinh^2 \varrho} \frac{\partial^2 \phi}{\partial \varphi^2} = 0. \tag{25}$$

For solving this wave equation, the standard procedure for this type of partial differential equation is to use the separation of variables method, and thus we take

$$\phi(t, \varrho, \varphi) = \phi_0(t) \, \phi_1(\varrho) \, \phi_2(\varphi). \tag{26}$$

The time dependence of the full potential ϕ is then given by $\phi_0(t)$ which will display a simple harmonic behavior, namely $\phi_0'' = -\omega^2 \phi_0$. It then follows that the time dependence has the structure $\phi_0(t) = A \cos(\omega t) + B \sin(\omega t)$. Moreover, to take advantage of the underlying rotational symmetry, we focus on the study of concentric wave propagation, and thus for the angular dependence it must hold $\phi_2' = 0$. As a result, all non-trivial behavior of the acoustic potential ϕ is contained in the remaining, radial dependence $\phi_1(\varrho)$. Summing up, to probe the prominent features of spacetime $\mathbb{D}_{\text{P}} \times \mathbb{R}$, the most suitable test waves are monochromatic concentric waves centered around the origin, so that the potential will take the final form

$$\phi(t, \varrho) = A^+ e^{i\omega t} \phi_1(\varrho), \tag{27}$$

where A^+ is the wave amplitude and ω its frequency.

Substitution of the wave potential, Eq. (27), into the wave equation, Eq. (25), and some simplification produces the ordinary differential equation describing all non-trivial radial behavior:

$$\phi_1'' + \coth \varrho \, \phi_1' + a^2 \frac{\omega^2}{c^2} \phi_1 = 0. \tag{28}$$

We found that the general analytic solutions of Eq. (28) are combinations of associated Legendre polynomials of the first and second type with complex arguments. However, apart from the lengthy exact results, we could derive the following, relatively simple and accurate, approximate solution for the radial dependence

$$\phi_1(\varrho) = e^{-\varrho/2} \left[A e^{\sqrt{1 - 4a^2\omega^2/c^2}\,\varrho} + B e^{-\sqrt{1 - 4a^2\omega^2/c^2}\,\varrho} \right]. \tag{29}$$

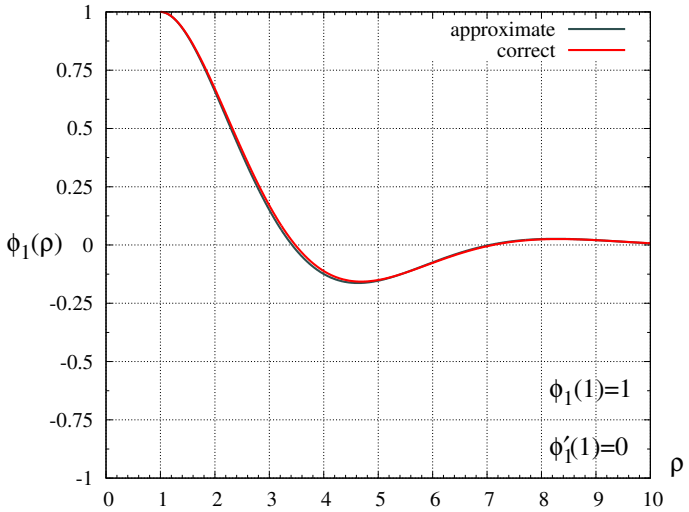

FIGURE 2 Non-trivial radial dependence of the acoustic potential for fixed scale $a = 1$, speed $c = 1$, frequency $\omega = 1$, with conditions $\phi_1(1) = 1$, $\phi_1'(1) = 0$. The correct analytic solution of Eq. (28) is marked red, and the approximation Eq. (29) is the plain black line.

Recall, that ω specifies the frequency of the monochromatic sound waves set up in the laboratory, whereas A and B are constants typically determined by the two boundary conditions on ϕ_1 and ϕ_1'. Moreover, in the formula consistent with wave acoustics the wave number $k = \omega/c$ emerges.

In the asymptotic limit $\varrho \to \infty$ ($r \to a$), the amplitude of oscillation decreases with time, *i.e.* damping occurs exponentially for the decaying sinusoidal wave, which can be read off directly from the approximation, Eq. (29). For the same limit, $\varrho \to \infty$, we have $\coth \varrho \to 1$ rather approaching fast, and the differential equation Eq. (28) also has solutions $\sim e^{-\varrho/2}$, exhibiting the same exponential damping. This damping or stretching of the wavelength can also been seen as an immediate consequence of the variable length calibration due to the underlying curved spacetime, see Eq. (7). Consequently it will never be possible for the wave to escape $\mathbb{D}_p$.

Also note that oscillatory wave behavior only surfaces when $\omega > \frac{c}{2a}$; this becomes evident from the bracketed terms of Eq. (29). Since physics dictates that the corresponding pressure for the acoustic potential is $p = -\varrho_0 \partial\phi/\partial t$, for this case the acoustic pressure wave will also be sinusoidal. On the other hand, for $\omega \leq \frac{c}{2a}$, no sinusoidal waves can materialize.

For the following numerical simulations, we assume $a = 1$, $c = 1$, and $\omega = 1 > 1/2$, so that harmonic wave features naturally will show up. Figure 2 captures exact and approximate results for the boundary conditions $\phi_1(1) = 1$ and $\phi_1'(1) = 0$. The corresponding absolute error is given in Figure 3 . This demonstrates that approximation Eq. (29) is exceptionally good, with an error ranging in this example between 2.65×10^{-8} and 0.018 (only when close to $\varrho = 3.4$).

For the next numerical simulation, we switch the boundary conditions to $\phi_1(1) = 0$ and $\phi_1'(1) = 1$, with all other parameters unchanged. The particle velocity of the acoustic wave is defined by $\boldsymbol{v} = \boldsymbol{\nabla}\phi$, which physically means that in this example the initial radial velocity is non-vanishing, opposed to the previous example. Figure 4 illustrates the behavior for the radial dependence ϕ_1, comparing exact results and approximated estimates. Again the approximation fares exceptionally well, and Figure 5 establishes that the maximum absolute error is roughly -0.044 occurring around $\varrho = 2.5$.

As a third and final example, we carry out a full wave simulation for the complete potential, Eq. (26), by using the first set of boundary conditions for the radial potential of Figure 2 . Besides, for this purpose, it will suffice to consider only the cosine mode of the harmonic time dependence. In a nutshell, this amounts to solving the boundary problem detailed in Figure 6 (with the previously assigned parameters for a, c and ω). As the concentric wave approaches the disk circumference at $\varrho \to \infty$ with increasing damping, the medium effectively has a fixed end at its border forming a node, and a standing wave will result. A graphical animation (based on the data provided in Figure 6) visualizes this effect [http://.....].[1]

[1] At this moment the media file with the animation (`PoincWave.avi`) is attached to the submission bundle. After a possible acceptance of this work, the publisher hopefully would provide a public link for access.

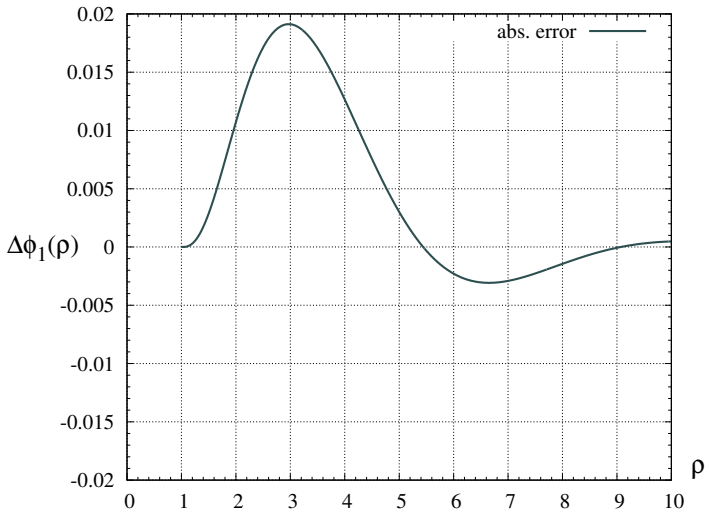

FIGURE 3 Absolute error between the approximate and exact result for the radial dependence of the acoustic potential, using fixed scale $a = 1$, speed $c = 1$, frequency $\omega = 1$, with conditions $\phi_1(1) = 1$, $\phi_1'(1) = 0$.

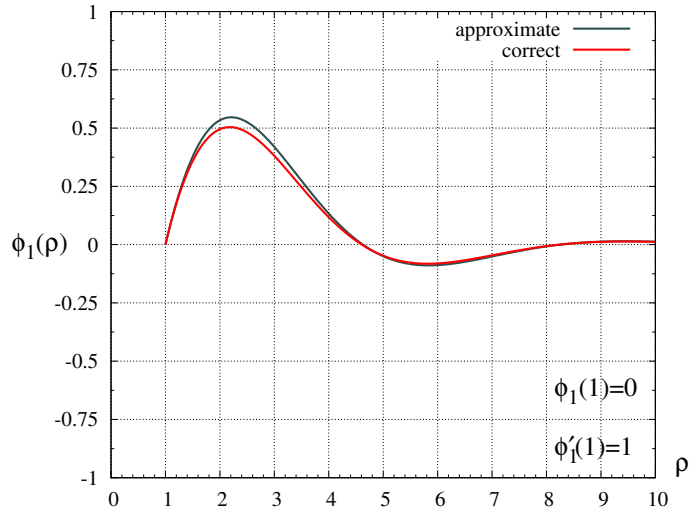

FIGURE 4 Non-trivial radial dependence of the acoustic potential for fixed scale $a = 1$, speed $c = 1$, frequency $\omega = 1$, with conditions $\phi_1(1) = 0$, $\phi_1'(1) = 1$. The correct analytic solution of Eq. (28) is marked red, and the approximation Eq. (29) is the plain black line.

Our examples served as an illustration, preserving as far as possible analytical results, but certainly other, fully numerical scenarios are conceivable, either by directly integrating the partial differential equation, Eq. (25), with numerical integrator software, or alternatively, simulating the acoustic parameters, Eq. (22), with finite-element methods in a virtual laboratory, see *e.g.* COMSOL Multiphysics®.[26]

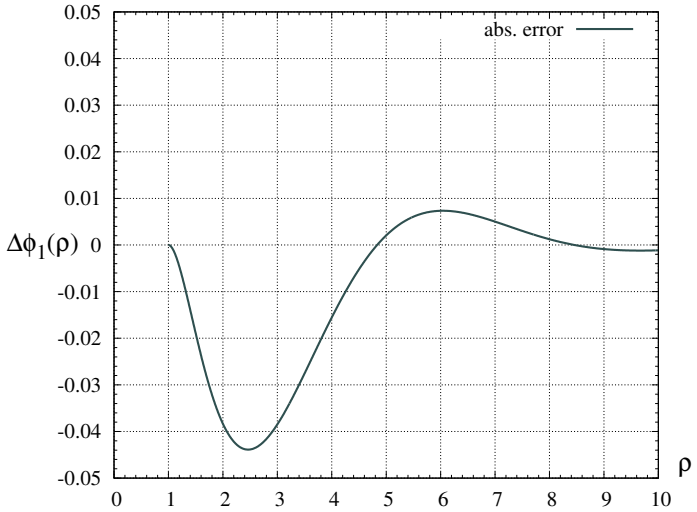

FIGURE 5 Absolute error between the approximate and exact result for the radial dependence of the acoustic potential, using fixed scale $a = 1$, speed $c = 1$, frequency $\omega = 1$, with conditions $\phi_1(1) = 0$, $\phi_1'(1) = 1$.

$$\boldsymbol{\Delta_M \phi = 0} \text{ on } \mathbb{D}_{\text{P}} = \underbrace{[0.4621, 0.9999]}_{r} \times \underbrace{[0, 2\pi[}_{\varphi},\ t \in [0, 4\pi]$$

first case: $\phi_1(1) = 1, \phi_1'(1) = 0$ with $\varrho \in [1, 10] \Leftrightarrow r \in [0.4621, 0.9999]$

$$\phi(0, r, \varphi) = 1 \text{ and } \frac{\partial}{\partial t}\phi(0, r, \varphi) = 0$$

solution: $\boldsymbol{\phi(t, r, \varphi) = \cos(\omega t)\, \phi_1(r)}$

one fixed endpoint for wave at $r \to a \ \Rightarrow$ standing wave

FIGURE 6 Boundary-value problem for a full simulation of acoustic wave propagation on the Poincaré disk $\mathbb{D}_{\text{P}}$. Fixed scale $a = 1$, speed $c = 1$, and frequency $\omega = 1$ remain unchanged.

5 | CONCLUSION

In this work, we have focussed on the implementation of hyperbolic geometry as defined by the Poincaré disk model within metamaterial acoustics. For the conventional gravity model, such a spacetime configuration would require exotic energy-matter, which is fundamentally impossible to attain. However, the acoustic analogue model of gravity is a more promising and practical candidate to be carried out in the laboratory. The corresponding constitutive relations reveal how the pertinent acoustic parameters have to be fine-tuned.

As a toy model, we have derived analytical solutions for concentric wave propagation probing the underlying spacetime structure. For achieving this aim, we also determined a useful class of approximating functions for the non-trivial radial dependence of the acoustic potential, which may be used effortlessly in all related numerical predictions. Not surprisingly, the waves are trapped within the disk and suffer a characteristic frequency shift when approaching its border. In this sense, it somehow resembles the futile attempt of a wave trying to escape a black hole from within which also experiences a redshift (although of distinct nature).

We do hope that the variational spacetime approach to transformation acoustics and the corresponding constitutive relations will establish itself as a compelling tool for the study and design of acoustic metadevices and may help to open up new research pathways in the field of metamaterials.

ACKNOWLEDGEMENTS

This work has been supported by the Spanish *Ministerio de Economía y Competitividad*, the European Regional Development Fund (ERDF) under grant TIN2017-89314-P, and the *Programa de Apoyo a la Investigación y Desarrollo 2018* (PAID-06-18) of the Universitat Politècnica de València under grant SP20180016. This work does not have any conflicts of interest.

References

1. Schattschneider Doris. The mathematical side of M.C. Escher. *Notices Am. Math. Soc.*. 2010;57:706–718.
2. Norris Andrew N.. Acoustic metafluids. *J. Acoust. Soc. Am.*. 2009;125(2):839–849.
3. Tung Michael M.. A fundamental Lagrangian approach to transformation acoustics and spherical spacetime cloaking. *Europhys. Lett.*. 2012;98:34002–34006.
4. Cummer Steven A.. Transformation Acoustics. In: Craster V. Richard, Guenneau Sébastien, eds. *Acoustic Metamaterials: Negative Refraction, Imaging, Lensing and Cloaking*, :197–218Springer Netherlands; 2013; Dordrecht.
5. Cummer Steven. A sound future for acoustic metamaterials. *J. Acoust. Soc. Am.*. 2017;141(5):3451.
6. Anderson James. *Hyperbolic Geometry*. London, UK: Springer-Verlag; 2005.
7. Kelly Paul, Matthews Gordon. *The Non-Euclidean, Hyperbolic Plane: Its Structure and Consistency*. New York, NY: Springer-Verlag; 2012.
8. Stahl Saul. *The Poincaré Half-plane: A Gateway to Modern Geometry*. Burlington, MA: Jones & Bartlett Publishers; 1993.
9. Tung Michael M., Peinado Jesús. A Covariant Spacetime Approach to Transformation Acoustics. In: Fontes Magnus, Günther Michael, Marheineke Nicole, eds. *Progress in Industrial Mathematics at ECMI 2012*, Mathematics in Industry, vol. 19: :335–340Springer, Berlin; 2014.
10. Tung Michael M., Weinmüller Ewa B.. Gravitational frequency shifts in transformation acoustics. *Europhys. Lett.*. 2013;101:54006–54011.
11. Tung Michael M., Weinmüller Ewa B.. Acoustic metamaterial models on the (2+1)D Schwarzschild plane. *J. Comput. Appl. Math.*. 2019;346:162–170.
12. Tung Michael M.. Modelling acoustics on the Poincaré half-plane. *J. Comput. Appl. Math.*. 2018;337:336–372.
13. Ungar Abraham A.. *Analytic Hyperbolic Geometry and Albert Einstein's Special Theory of Relativity*. Singapore: World Scientific; 2008.
14. García Alberto A., Hehl Friedrich W., Heinicke Christian, Macias Alfredo. The Cotton tensor in Riemannian spacetimes. *Class. Quantum Gravity.* 2004;21(4):1099–1118.
15. Visser Matt, Barceló Carlos, Liberati Stefano. Analogue models of and for gravity. *Gen. Rel. Grav.*. 2002;34:1719–1734.
16. Sakoda Kazuaki. *Electromagnetic Metamaterials: Modern Insights into Macroscopic Electromagnetic Fields*. Singapore: Springer; 2019.
17. Cai Wenshan, Shalaev Vladimir. *Optical Metamaterials: Fundamentals and Applications*. Basel: Springer International; 2020.

18. Romero-García Vicente, Hladky-Hennion Anne-Christine. *Fundamentals and Applications of Acoustic Metamaterials: From Seismic to Radio Frequency*. Hoboken, NJ: Wiley & Sons; 2019.

19. Shelby R. A., Smith D. R., Schultz S.. Experimental verification of a negative index of refraction. *Science*. 2001;292:77–97.

20. Pendry John B.. Negative refraction makes a perfect lens. *Phys. Rev. Lett.*. 2000;85:3966-9.

21. Zhang Xiang, Lui Zhaowei. Superlenses to overcome the diffraction limit. *Nat. Mater.*. 2008;7(6):435–441.

22. Leonhardt Ulf, Smith David R.. Focus on cloaking and transformation optics. *New J. Phys.*. 2008;10(11):115019.

23. Cummer Steven A., Schurig David. One path to acoustic cloaking. *New J. Phys.*. 2007;9(3):45–52.

24. Mechel Fridolin P.. *Formulas of Acoustics*. Berlin: Springer-Verlag; 2002.

25. Rosenberg Stephen. *The Laplacian on a Riemannian Manifold: An Introduction to Analysis on Manifolds* London Mathematical Society Student Text, vol. 31: . Cambridge, UK: Cambridge University Press; 1997.

26. COMSOL AB, Stockholm, Sweden `http://www.comsol.com`. COMSOL Multiphysics®.